APS physics

CHORUS

This is the accepted manuscript made available via CHORUS. The article has been published as:

Spectroscopic prescription for optimal stimulated Raman transfer of ultracold heteronuclear molecules to the lowest rovibronic level

Jin-Tae Kim, Yonghoon Lee, Bongsoo Kim, Dajun Wang, William C. Stwalley, Phillip L. Gould, and Edward E. Eyler

Phys. Rev. A **84**, 062511 — Published 21 December 2011

DOI: 10.1103/PhysRevA.84.062511

Spectroscopic Prescription for Optimal Stimulated Raman Transfer of Ultracold Heteronuclear Molecules to the Lowest Rovibronic Level

Jin-Tae Kim,[1] Yonghoon Lee,[2] Bongsoo Kim,[3,*] Dajun Wang, [4,†] William C. Stwalley,[4,*] Phillip L. Gould,[4] and Edward E. Eyler[4]

[1]Department of Photonic Engineering, Chosun University, Gwangju 501-759, Korea,

[2]Department of Chemistry, Mokpo National University, Jeonnam, 534-729, Korea,

[3]Department of Chemistry, KAIST, Daejeon 305-701, Korea, and [4]Department of Physics, University of Connecticut, Storrs, CT 06269, USA

Abstract

We show that the multiplicative product (MB×UM) of a molecular beam excitation spectrum (MB) and an ultracold molecule excitation spectrum (UM), with a frequency offset appropriate to the initial ultracold molecule level, provides the relative rate of stimulated Raman transfer (SRT) from a given high rovibrational level to the lowest rovibronic level, i.e. the $v''=0, J''=0$ level of the ground electronic state for photoassociated (and magnetoassociated) ultracold molecules. This product spectrum clearly indicates the optimal pathways for SRT, even when the two component spectra are completely unassigned. We illustrate this specifically for the case of KRb.

[*]E-mail: bongsoo@kaist.ac.kr, w.stwalley@uconn.edu

[†]Present address: Department of Physics, The Chinese University of Hong Kong, Shatin, Hong Kong

I. **Introduction**

Ultracold molecules (UM) have attracted growing interest in recent years, due in large part to their potential utility in areas such as ultracold chemistry [1-3], quantum dipolar systems [4, 5], quantum information [6], and tests of fundamental symmetries [7]. In order to achieve the lowest temperatures, the molecules are formed by binding together atoms that are already ultracold, using either photoassociation (PA) [8-14] or magnetoassociation (MA) [15-16]. In PA, laser light transfers a colliding atom pair from the ground-state continuum to an excited bound state, followed by spontaneous emission (SE) into a bound level of the $X\ ^1\Sigma^+$ electronic ground state or the metastable $a\ ^3\Sigma^+$ state correlating to two ground state atoms. In MA, a magnetic field is swept through a Feshbach resonance that couples the free-atom continuum to a bound molecular state. In the case of PA, either 100% or ~ 75% of the population ends up in the $a\ ^3\Sigma^+$ state and 0% or ~ 25% ends up in the $X\ ^1\Sigma^+$ state, depending on whether $\Omega = 0^-$ or 2 or $\Omega = 0^+$ or 1, respectively [17]. In the case of MA, 100% of the molecules are in the $a\ ^3\Sigma^+$ state [18]. Hence our emphasis here is on transfer from the $a\ ^3\Sigma^+$ state to the $v'' = 0, J'' = 0$ level of the X state, denoted here as $X(0, 0)$. Note that for such triplet-to-singlet transfer, an intermediate state of strongly mixed singlet-triplet character will be optimal.

A disadvantage of these long-range association techniques is that the resulting molecules typically reside in near-dissociation vibrational levels of the X or a states, although exceptions [10, 19-21] do exist. These high vibrational levels are problematic for two reasons: 1) they are not stable against vibrational quenching (inelastic and reactive collisions with atoms or other molecules); and 2) the electric dipole moments of heteronuclear molecules, which are important for many of the applications, are

vanishingly small in these barely-bound levels. Transferring UM from their initial high rovibrational levels into the rovibrational ground state, while keeping them translationally cold, is therefore of critical importance.

Driving a stimulated Raman transition through an electronically excited state is an obvious way to realize this population transfer, ideally via stimulated Raman adiabatic passage (STIRAP) with nearly 100% efficiency [22]. Here, we present a spectroscopic prescription for optimizing this transfer. An excited intermediate state is required that has strong couplings both to the initial high-v level (Stokes (PUMP) transition) and to the final $X(0,\ 0)$ level (anti-Stokes (DUMP) transition). In principle, if the molecular potentials and the energy levels of the electronic states are well known, the relevant Franck-Condon factors (FCFs) between relevant electronic states can be calculated, so that optimal rovibronic levels may be chosen for the population transfer. However, this is not always possible due to a scarcity of spectroscopic information for particular molecules. Also, severe perturbations among the electronic states can make it difficult to fully analyze the spectra, to accurately calculate the transition dipole matrix elements between states, and thus to choose optimal routes for transfer.

Alternatively, various techniques such as Feshbach-optimized photoassociation (FOPA) [23] and resonant coupling of excited states due to electronic coupling [24] have been developed to avoid the SRT. These methods, however, also require detailed spectroscopic information and complex calculations to predict population transfer rates, and are not yet experimentally realized.

The primary method used to date to identify SRT pathways is that of dark resonances [25]. In SRT, the PUMP transition is first found by observing the depletion of the high-v

molecules on resonance with strong transitions to intermediate levels. With this resonant PUMP light present, the DUMP transition is then found by minimizing the depletion when the PUMP and DUMP light are two-photon resonant, resulting in a coherent dark-state superposition of initial and final states. These high-resolution spectroscopic methods have allowed pathways to be identified for efficient transfer to $X(0, 0)$ in KRb [15], Cs_2 [26], and Rb_2 [27]**.** Earlier relatively inefficient incoherent schemes were used to produce $X(0, 0)$ in K_2 [13] and RbCs [14]. A related scheme using optical pumping (spontaneous Raman transitions) with broadband light has also been implemented in Cs_2 [28].

In the present work, we describe an alternative method for straightforward identification of the optimum pathways for SRT in heteronuclear alkali diatomic molecules. It combines pulsed-laser resonance-enhanced multiphoton ionization (REMPI) spectroscopy of ultracold high-v molecules in the X or a states produced by PA (UM) with pulsed-laser REMPI spectroscopy of $X(0, 0)$ molecules in a pulsed supersonic molecular beam (MB) [29-32]. These two independent spectra, starting from different initial states, are configured to probe the same excited-state energy range. The key is then to offset the two spectra by the difference in their initial binding energies and then take their multiplicative product.

The connection with optimal SRT pathways can be explained by using a succinct mathematical equation. Consider the intensity I(SRT) of SRT from a high rovibrational level (v, J) of the $a\ ^3\Sigma^+$ state of KRb to the $X(0, 0)$ level of the $X\ ^1\Sigma^+$ state via a near-resonant intermediate state e' in rovibrational level (v', J'). Close to a single resonance,

$$I(\mathrm{SRT}) \propto \left|\left\langle a, v, J \left| D_{ae'} \right| e', v', J' \right\rangle\right|^2 \times \left|\left\langle e', v', J' \left| D_{e'X} \right| X, v'' = 0, J'' = 0 \right\rangle\right|^2, \qquad (1)$$

where D_{ij} is the electronic transition dipole moment (ETDM) function between electronic states $|i\rangle$ and $|j\rangle$ and the bra and ket vectors refer to the rovibrational wavefunctions.

However, the first matrix element squared is also proportional to the intensity of the excitation spectrum to the e' intermediate state of an UM formed by PA or MA in the (v, J) level of the a state, i.e. to I(UM). Moreover, the second matrix element squared is proportional to the excitation spectrum to the e' intermediate state of $v'' = 0$, low-J'' levels of the X ground electronic state, i.e. to the dominant features in I(MB). Thus, at the same total level energy E where one observes the same intermediate state $e'(v', J')$ in both spectra, the relative strength of various SRT pathways can be easily obtained by simply taking the product of the intensities, $I(\mathrm{SRT}) \propto I(\mathrm{MB}) \times I(\mathrm{UM})$.

An important advantage of this method is that the generally complex spectra of the excited intermediate levels need not be assigned, greatly simplifying the procedure. In fact the intermediate levels need not even be identified — the optimization is strictly empirical. For a given initial (high-v) level and the final $X(0, 0)$ level, the product spectrum automatically determines the optimal intermediate level for SRT. The technique takes advantage of the strengths of the two types of spectroscopy. Ultracold PA or MA produces primarily high-v molecules as the starting point, while the MB is a source of predominantly $X(0, 0)$ molecules.

It should also be noted that the $X(0, 0)$ levels have hyperfine structure, and a specific hyperfine component must be selected to produce a gas of identical molecules in a single quantum state [15]. However, we do not consider this complication here.

II. Experimental Methods

This scheme can be employed for diatomic molecules with an arbitrary combination of different alkali atoms, as well as many other cases not yet studied. Figure 1 shows the *ab initio* potential energy curves (PECs) [33], the primary energy levels, and processes involved in our MB, PA, and UM experiments relevant to transferring population from high rovibronic levels of the $X\,^1\Sigma^+$ or the $a\,^3\Sigma^+$ state to the $X(0, 0)$ level of the KRb molecule.

The PA process followed by SE prepares molecules in high rovibrational levels of the $X\,^1\Sigma^+$ and $a\,^3\Sigma^+$ states. These levels become the initial long-range levels for the UM excitation spectrum. Initial levels for the MB excitation spectra are low rotational levels, predominantly in the $v'' = 0$ vibrational level of the $X\,^1\Sigma^+$ state near the equilibrium internuclear distance R_e, which are prepared by supersonic expansion of K and Rb vapor with an inert carrier gas.

A one-color resonance-enhanced two photon ionization (RE2PI) detection method is used to obtain the MB and UM excitation spectra. For efficient population transfer to $X(0, 0)$, a suitable intermediate level $e'(v', J')$, represented in Fig. 1 as a horizontal dashed line, should be selected. An ideal intermediate level for the optimal SRT pathway has large ETDMs and large FCFs with both the initial near-dissociation level in the large internuclear distance region and the final level in the X state equilibrium internuclear distance region. Thus, a large multiplicative product of a MB excitation spectrum and an UM excitation spectrum to the same intermediate level provides a large SRT rate from a given high rovibrational level $a(v, J)$ to $X(0, 0)$.

The following pulsed supersonic MB and UM experiments are used to carry out the methods explained above.

A. Pulsed Supersonic MB Experiment

A pulsed supersonic MB of alkali molecules with a rotational temperature of less than 5 K is generated by a pulsed jet, preparing a small number of significantly populated levels; typically for recent KRb experiments [30] the dominant features involve $X(0, J'')$ levels with traces of $X(1, J'')$ for low J''. KRb molecules were produced by expanding K (^{39}K and ^{41}K) and Rb (^{85}Rb and ^{87}Rb) vapor with Kr gas through a 300^{o}C pulsed nozzle, with a backing pressure of 530–550 torr, into a vacuum chamber. The pulsed jet was collimated by a 1.2 mm diameter skimmer.

Although four different isotopologues (^{39}K^{85}Rb, 67.3%; ^{39}K^{87}Rb, 26.0%; ^{41}K^{85}Rb, 4.9%; ^{41}K^{87}Rb, 1.9%) are typically present, their spectra can be distinguished using isotopic relationships, e.g. mass-reduced quantum numbers. In our MB experiment, we record excitation spectra of KRb by one-color RE2PI. Two photons from a Nd:YAG laser pumped dye laser resonantly excite and ionize the KRb. The ion signal at the mass-to-charge ratio m/Z = 124 (^{39}K^{85}Rb) is well separated from the signal of other less prevalent isotopologues (^{39}K^{87}Rb and ^{41}K^{85}Rb) by use of a linear time-of-flight mass spectrometer, with a dual microchannel plate detector ($m / \Delta m \approx 500$). Since our goal is to end up in X(0, 0), the $X(0, J'')$ absorption spectral intensities give us the intensity of the second step of the SRT (SR2) in Fig. 1 from a variety of possible intermediate states.

B. PA and UM Experiments

Ultracold $^{39}K^{85}Rb$ molecules with nonzero dipole moments are formed by PA [12] in overlapped ^{39}K and ^{85}Rb dark-spot magneto-optical traps (MOTs) with densities of 3×10^{10} cm^{-3} and 1×10^{11} cm^{-3} and temperatures of 300 μK and 100 μK, respectively. A cw PA laser is applied to generate a specific rovibrational level of the excited molecular $3(0^-)$ state near the K($4s$) + Rb($5p_{1/2}$) asymptote. This state decays exclusively to the $a\ ^3\Sigma^+$ ($\Omega = 0^-$ and 1) state due to the electric dipole transition selection rules with respect to the total parity and angular momentum ($\Delta\Omega = 0,\ \pm1,\ + \leftrightarrow +,$ and $- \leftrightarrow -$) [34]. High-resolution PA of the ultracold atoms involves free-to-bound absorption from colliding ultracold atoms to high vibrational levels of excited electronic states with only a few quanta of rotational angular momentum ($J' < 5$ in our KRb spectra [12]).

For detection of these high-v levels, a pulsed dye laser beam with 0.2 cm^{-1} linewidth, ~ 5 ns pulse width, 10 Hz repetition rate, and a few mJ pulse energy illuminates the overlapped MOTs to provide state-selective RE2PI. The KRb^+ ions produced are accelerated into a Channeltron ion detector. This RE2PI detection reveals the first step of the SRT, labeled SR1 in Fig. 1.

III. Results and Discussion

For the important case of $^{39}K^{85}Rb$, the many mutually perturbing states arising from the K + Rb($5p$) and K($4p$) + Rb asymptotes [33] make the full assignment of the spectrum difficult. In the spectroscopic region given as an example here (15372 - 15562 cm^{-1}), the levels of most states are complex mixtures of Σ and Π character, and of singlet and triplet character, and the fractional parentage of given electronic states can

vary rapidly with energy. Thus the energy levels in this region have not previously been assigned.

First, in the next two subsections, we briefly describe spectral analyses obtained from the MB and UM excitation spectra in Fig. 2(a) and Fig. 2(b), respectively, for the case of $^{39}K^{85}Rb$. Second, in the third subsection, we discuss the new method of MB×UM product spectroscopy, shown in Fig. 2(c), for determination of the optimal pathway for SRT of high-v levels of $^{39}K^{85}Rb$ to the lowest rovibronic level. Finally, in the fourth subsection we discuss applications of our method to other heteronuclear diatomic molecules.

A. The Pulsed Supersonic MB Excitation Spectra

The pulsed supersonic MB generates molecules with vibrational temperature near 1 K for KRb, which means that the population is ~ 95% in $v''=0$ and ~ 5% in $v''=1$. We expect that transitions between the singlet ground state and singlet intermediate states will appear as the main transitions in the RE2PI spectrum from MB. Due to the perturbations between the singlet and triplet states, however, both the intermediate triplet and singlet states can be reached from the initial ground state populated by the supersonic MB. However, since the X state is of Σ^+ ($\Omega=0^+$) symmetry, only $\Omega=0^+$ and 1 states can be accessed in these spectra considering the transition selection rules for $\Delta\Omega$ and parity.

We have been able to assign nearly all of the observed transitions by analyzing both the MB and UM spectra, although these assignments are not necessary or even particularly useful for finding the optimal SRT path. Detailed analysis for the quantum number assignments, vibrational spacings, etc. of the relevant electronic states is reported

in a separate paper [35].

In our experimental region *ab initio* PECs [33] are available for all of the states, $A\,^1\Sigma^+, 3\,^1\Sigma^+, 1\,^1\Pi, 2\,^3\Sigma^+$, and $b\,^3\Pi$, that lie below the K + Rb ($5p_{1/2}$) dissociation asymptote. A MB spectrum for $^{39}K^{85}Rb$ is given in Fig. 2(a), with assignments to four of these states. The singlet-singlet transitions ($1\,^1\Pi \leftarrow X\,^1\Sigma^+$) appear as the main strong features of this spectrum. Transitions assigned to MB ($1\,^1\Pi(v') \leftarrow X\,^1\Sigma^+(v''=0)$) are identified by considering the corresponding FCFs calculated using the *ab initi*o PECs, the term energies observed by Okada *et al.* [36] and Kasahara *et al.* [37], and the ETDMs reported by Beuc *et al.* [38]. Singlet transitions to the $A\,^1\Sigma^+$ state are not observed due to small FCFs between the X and $A\,^1\Sigma^+$ states. According to Beuc *et al.*, the $1\,^1\Pi \leftarrow X\,^1\Sigma^+$ transition among the various $(1-4)\,^1\Sigma^+ \leftarrow X\,^1\Sigma^+$ transitions, is predicted to have the largest ETDM, particularly around R_e of the $X\,^1\Sigma^+$ state. Also, the ETDM of the $3\,^1\Sigma^+ \leftarrow X\,^1\Sigma^+$ transition is predicted to be very small, but we nevertheless observe regular and very weak vibronic structure assignable to the $3\,^1\Sigma^+(v') \leftarrow X\,^1\Sigma^+(v''=0)$ transitions in the MB excitation spectrum.

The triplet states can only be accessed through the perturbations between singlet and triplet states because the initial state in the MB experiment is the singlet $X\,^1\Sigma^+$ state. Thus these transitions ($2\,^3\Sigma^+$ and $b\,^3\Pi \leftarrow X\,^1\Sigma^+$) are weak except when there is strong spin-orbit mixing between the singlet and triplet states.

It is normally easy to distinguish between the singlet and triplet states because the $1\,^1\Pi\ (\Omega=1)$ state accessible in this energy region has only one Ω component while the

triplet $2\,^3\Sigma^+$ ($\Omega = 0^-$ and 1) and $b\,^3\Pi$ ($\Omega = 0^{\pm}$, 1, and 2) states have multiple components. However, only the $\Omega = 1$ component of the triplet $2\,^3\Sigma^+$ and $b\,^3\Pi$ states was observed in the MB spectra shown in Fig. 2(a) considering the perturbation selection rule. Both the $\Omega = 0^-$ and the $\Omega = 1$ components of the $2\,^3\Sigma^+$ state can be accessed from the initial $a\,^3\Sigma^+$ state using the UM method as discussed below. It is impossible to identify the $\Omega = 0^-$ and $\Omega = 1$ components by either the UM method alone or the MB method alone because the energy ordering of those states cannot be identified. However, we can readily identify the $\Omega = 1$ state from the MB experiment by comparing the MB spectra in Fig. 2(a) with the UM spectra in Fig. 2(b). Also the $2\,^3\Sigma^+$ state, with fewer Ω components and with separations between its components smaller than those of the $b\,^3\Pi$ state, can readily be distinguished from the $b\,^3\Pi$ state. After the $1\,^1\Pi$, $b\,^3\Pi$, and $2\,^3\Sigma^+$ states are assigned, only one regular vibronic progression with very weak signal intensities (which are smaller than those of $v'' = 1$ bands related to the strong $v'' = 0$ signals) are not yet assigned. The vibrational spacing of this progression (~ 39 cm^{-1}) is close to that calculated for the $3\,^1\Sigma^+$ state. Thus we assign this progression as the $3\,^1\Sigma^+$ state ($v' = 28 - 52$). We will report detailed information on this state in another publication.

In the MB RE2PI spectrum (Fig. 2(a)), the vibrationally hot $v' \leftarrow v'' = 1$ bands are very weak compared to the $v' \leftarrow v'' = 0$ bands. The analysis of these hot bands indicates that the vibrational temperature $T_{vib.} < 1$ K. In our spectra the separate rotational lines for each vibrational level were not resolved. The $1\,^1\Pi(v' = 11) \leftarrow X\,^1\Sigma^+(v'' = 0)$ band observed in our MB RE2PI spectrum and a simulation using the parameters ($T_{rot.}$ =

1.490(49) K, Gaussian linewidth = 0.1111(36) cm^{-1}, band origin = 15677.1992(31) cm^{-1}, rotational constant = 0.02722(13) cm^{-1}) compare well, as shown in Fig. 3.

B. The UM Excitation Spectra

In the heteronuclear case of KRb, the emission from a chosen level of an upper electronic state of a PA line is either to both the *X* and *a* states (for $\Omega = 0^+$ or 1 states), or to the *a* state only (for $\Omega = 0^-$ or 2 states) to the *a* state. It is from these highly-excited *a* or *X* rovibrational levels to various intermediate excited rovibronic levels that the first step of an SRT (SR1) to *X*(0, 0) would take place. However, the intermediate states are generally well below the near-dissociation region of the excited states reached by PA; moreover the absorption spectra of these high *a* or *X* levels can be distinct from the absorption spectra of colliding atoms (i.e. PA) since the lower state wavefunctions can be significantly different. The intensities in these spectra are directly proportional to the intensity of the first step (SR1) of a SRT through an intermediate electronically excited state to the *X*(0, 0).

An example of an UM spectrum for KRb (produced by PA to a level of the excited $3(0^-)$ state followed by SE to the *a* state) is shown in Fig. 2(b). It should be noted that the energy scales in both the MB and the UM spectra are the same. However, the frequency axis of the UM spectrum shown Fig. 2(b) is shifted up by the energy difference $E(a, v = 21, J = 0) - E(X, v'' = 0, J'' = 0)$. This causes transitions from the lower level in Fig. 2(a) [*X*(0, 0)] and the lower level in Fig. 2(b) [*a*(21, 0)] to a common upper level to coincide. This assumes that the energies of the *a*(*v*, *J*) levels are known with respect to *X*(0, 0). Fortunately these levels are relatively unperturbed and readily assigned; they are

well known for KRb and most other cases of heteronuclear alkali dimers thanks to the work of Tiemann's group [39].

Considering only the spectroscopic spin selection rule, one might think that the triplet-triplet transitions will appear as the main transitions in the RE2PI spectrum of the UM experiment because the initial state is the triplet $a\ ^3\Sigma^+$ state. However, the *a* state is better described in Hund's case (c) as a state of $\Omega = 0^-$ and 1 character, as discussed in the next paragraph. The vibronic structures observed in the UM and MB excitation spectra are significantly different from each other. This is mainly because the electron-spin characters of the initial states of the UM ($a\ ^3\Sigma^+$) and MB ($X\ ^1\Sigma^+$) excitation spectra and the shapes (and locations) of the corresponding PECs are very different. The main features of the MB RE2PI spectrum from UM ($2\ ^3\Sigma^+ \leftarrow a\ ^3\Sigma^+$ and $b\ ^3\Pi \leftarrow a\ ^3\Sigma^+$) are identified by considering the corresponding FCFs calculated using the *ab initi*o PECs, the number of the Ω components of states observed in the MB and UM experiments, the separation between the Ω components of the triplet states, and the ETDMs reported by Beuc *et al.* [38].

In contrast to the MB spectra, the UM spectra show strong transitions to both singlet and triplet states. Since the *a* state includes both $\Omega = 0^-$ and 1 components, absorption can occur to states with $\Omega = 0^-, 0^+, 1,$ and 2, i.e. to all states correlating to the K + Rb(5*p*) and K(4*p*) + Rb asymptotes. The UM spectra are therefore more congested. The $3\ ^1\Sigma^+$ state is not observed in the UM experiment when a PA line of the $3(0^-)$ state, which decays to only the $a\ ^3\Sigma^+$ state, is used; however, this state is observed when a PA line of the $3(0^+)$ state is used [40].

The UM spectra also have broader FCF distributions than the MB spectra, which are localized in a small region. Because the MB spectra also contain only $\Omega = 0^+$ and 1 states, it is easier to assign the electronic states than in the UM spectra. However, it is still not easy to assign the electronic states by using only the MB spectra if there are severe perturbations among the electronic states. Comparison with the UM spectra makes it possible to observe $\Omega = 0^-$ and 2 components of the $2\,^3\Sigma^+$ and $b\,^3\Pi$ states forbidden from the $X\,^1\Sigma^+$ state and to unravel these complex and highly perturbed spectra.

C. MB×UM Product Spectroscopy

Figures 2(a), (b), and (c) show the intensities of the MB spectra, the UM spectra, and the multiplicative product MB×UM spectra, respectively. We show here that this provides a reliable determination of the relative rates of SRT to the target $X(0, 0)$ level via a variety of intermediate levels, even if the assignment of these levels is unknown. The strongest lines in this product spectrum for both the intermediate triplet and singlet states are marked by α, β, γ, and δ. These represent the most favorable routes for population transfer from $a(v, J)$ to $X(0, 0)$. Two of the intermediate levels, α and δ, are identified as the $2\,^3\Sigma^+ (\Omega = 1)$ $v' = 44$ and 45 levels. The others, β and γ, are identified as the $1\,^1\Pi$ $v' = 7$ and 8 levels, respectively. In particular, the intermediate level γ is found to provide the most efficient population transfer route, $a\,^3\Sigma^+ (v = 21) \rightarrow 1\,^1\Pi (v' = 8) \rightarrow X\,^1\Sigma^+ (v'' = 0)$. We emphasize that although here we have been able to assign the intermediate levels, this is not necessary for the optimization of SRT. Moreover, the product spectrum in Fig. 2(c) is relevant only to SRT from $v = 21$

of the *a* state. To optimize SRT from a different *v* in the *a* state with a different UM spectrum, we would simply need to change frequency offset, in accord with the different binding energy for the new *v* level, before multiplying the same MB spectrum times the new UM spectrum.

The vibrational spacing $\Delta G_{v'+1/2=7.5}$ $(= G_{v'=8} - G_{v'=7})$ of the $1\,^1\Pi$ state [35] as shown in Fig. 4 is remarkably small compared to the adjacent values due to spin-orbit interactions between the electronic states. The singlet-triplet mixing among the $\Omega = 1$ states ($1\,^1\Pi, 2\,^3\Sigma^+ (\Omega = 1)$, and $b\,^3\Pi$ ($\Omega = 1$)) is particularly strong in this excitation energy region where the strong α, β, γ, and δ peaks of the MB×UM product spectrum are located. It is this strong singlet-triplet mixing in the intermediate level that leads to efficient population transfer to $X(0, 0)$.

Two recent experiments have applied SRT to the case of KRb. The experiments by Ospelkaus *et al.* [15] reach SRT efficiencies over 90% from the initial magnetoassociated (Feshbach) molecule with primarily triplet character to the rovibrational ground state ($X(0, 0)$) in a high phase space density gas of KRb molecules. However, they used a near infrared laser beam wavelength which is not in the strongly perturbed region studied here. We expect that if we were to study their transfer region, we would identify their intermediate transfer level to $X(0, 0)$. Aikawa *et al.* [40] employed SRT in KRb to the lowest rovibronic level ($X(0, 0)$) from weakly bound levels of the *X* state (formed by PA) and thus used an essentially pure singlet level as the intermediate state. Our product method would work equally well in identifying optimal intermediate states using the same MB spectrum and a new UM spectrum from a high-*v* level of the *X* state. However, in this singlet-singlet SRT, a strongly perturbed intermediate state is no longer desirable.

D. Applications to other diatomic molecules

Our new method can also be applied to homonuclear alkali diatomic molecules. In the homonuclear case, the emission of *gerade* excited states is to the *ungerade a* state, while the emission of *ungerade* excited states is to the *gerade X* state. Due to this difference in the symmetry with respect to the inversion center, these two *X* and *a* states cannot have common upper states assuming electric-dipole-allowed transitions, and cannot be coupled by a SRT (except possibly by hyperfine mixing of the *X* and *a* states extremely close to dissociation as in MA). Thus the high-lying rovibrational levels of the *X* state with *gerade* symmetry near the dissociation limit of the ground state and intermediate electronic states with *ungerade* symmetry are needed to transfer the population to $X(0, 0)$. Thus only high-v levels of the *X* state (and not the *a* state) can be transferred by SRT to $X(0, 0)$.

Let us now focus on other heteronuclear molecules. Among heteronuclear alkali diatomic molecules, RbCs is a promising candidate because spectra from both MB and UM experiments are available with visible laser frequencies. Although PA and incoherent transfer to the ground state were carried out in 2004 by Kerman *et al*. [8], there has yet been no transfer to $X(0, 0)$ by SRT. This reflects the fact that efficient transfer routes to $X(0, 0)$ are still not known. Debatin *et al.* [25] used dark-state spectroscopy to investigate the intermediate $A\,^1\Sigma^+ \sim b\,^3\Pi$ states, mixed by spin-orbit interaction for transferring RbCs Feshbach molecules to $X(0, 0)$. Also recent UM experiments in the DeMille group [41] have been carried out with high resolution in the 640 nm region to investigate intermediate states for transferring to the $X(0, 0)$ level. MB experiments near 640 nm [29] and 500 nm [30] from the lowest vibrational level of the *X* state for RbCs have been

carried out. Unfortunately the intermediate region between 640 nm and 500 nm is not yet available. The existing UM spectra [41] show significant hyperfine structure. However, we expect that it may be possible to combine the MB and UM spectra after deconvolution of the rotational structure and hyperfine structure. Then our MB×UM product spectra can be used to identify appropriate SRT routes near 640 nm.

Although the MB spectra (Fig. 1 in Ref. 29) are simpler than those obtained by other experimental methods, they could not be assigned to the vibrational levels of the specific electronic states because vibrational progressions for the electronic states in that region are not regular, due to large perturbations among the electronic states. However, if we use our new methodology, that severely perturbed region should identify optimal transfer routes to $X(0, 0)$ due to strong singlet-triplet mixing with the intermediate states, because the final state is a singlet state while the initial state is a triplet state.

The MB×UM method should also be very useful for other alkali heteronuclear diatomic molecules such as LiK [9], LiCs [10], and NaCs [11], for which PA has been carried out. Also, there are many other molecules such as KCs, LiAl, and IBr, for which PA has not carried out and for which both singlet and triplet states can be formed in the asymptotic limit of two atoms with a ^2S or ^2P atomic ground state. Molecules formed from atoms with spin > ½ should also be amenable to similar treatment.

IV. Summary

In summary, we introduce a new method, MB×UM product spectroscopy, for reliably identifying pathways suitable for STIRAP transfer of ultracold molecules to the lowest rovibronic level, $X(0, 0)$. Unlike previous methods, it is unnecessary to make detailed

spectroscopic assignments of the intermediate states used for transfer. Furthermore, this method provides a powerful spectroscopic tool for exploring complex spectra which cannot readily be analyzed by using the spectra from either MB and UM experiments alone. Finally, we have determined that in $^{39}K^{85}Rb$ the most efficient route to transfer molecules formed near dissociation by PA to the lowest rovibronic levels of the $X\,^1\Sigma^+$ ground electronic state is through the path $a\,^3\Sigma^+(v=21) \rightarrow 1\,^1\Pi(v'=8) \rightarrow X\,^1\Sigma^+(v''=0)$.

Similar considerations apply to other heteronuclear alkali dimers and other systems where the dissociation energy of the $X(0, 0)$ level and the binding energy of the UM level are precisely known. It can also be used to improve the accuracy of the dissociation energy or the binding energy if one of the two quantities is accurately known.

Acknowledgement

This research was supported at Chosun University (2009-0085319) and at KAIST (2009-0083138) by NRF in Korea, and at UConn by the National Science Foundation (PHY-0855613) and by the Air Force Office of Scientific Research (MURI FA9550-09-1-0588). Y. Lee thanks the Institute for Basic Science of Mokpo National University. J. T. Kim and W. C. Stwalley thank D. DeMille for interesting discussions on RbCs.

References

(1) S. Ospelkaus *et al.*, Science. **327**, 853 (2010).

(2) J. J. Zirbel *et al.*, Phys. Rev. Lett. **100**, 143201 (2008).

(3) G. Quéméner and J. L. Bohn, Phys. Rev. A **83**, 012705 (2011).

(4) K.-K. Ni *et al.*, Nature **464**, 1324 (2010).

(5) G. M. Bruun and E. Taylor, Phys. Rev. Lett. **101**, 245301 (2008).

(6) D. DeMille, Phys. Rev. Lett. **88**, 067901 (2002).

(7) D. DeMille *et al.*, Phys. Rev. Lett. **100**, 023003 (2008).

(8) A. J. Kerman *et al.*, Phys. Rev. Lett. **92**, 033004 (2004).

(9) A. Ridinger *et al.*, Europhysics Lett. **96**, 33001 (2011).

(10) J. Deiglmayr *et al.*, Phys. Rev. Lett. **101**, 133004 (2008).

(11) C. Haimberger *et al.*, Phys. Rev. A **70**, 021402 (2004).

(12) D. Wang *et al.*, Phys. Rev. Lett. **93**, 243005 (2004).

(13) A. N. Nikolov *et al.*, Phys. Rev. Lett. **84**, 246 (2000).

(14) J. M. Sage *et al.*, Phys. Rev. Lett. **94**, 203001 (2005).

(15) S. Ospelkaus *et al.*, Phys. Rev. Lett. **104**, 030402 (2010).

(16) C. Chin, R. Grimm, and P. S. Julienne, Rev. Mod. Phys. **82**, 1225 (2010).

(17) D. Wang *et al.,* Eur. Phys. J. D **31**, 165 (2004).

(18) W. C. Stwalley, Eur. Phys. J. D **31**, 221 (2004).

(19) C. Gabbanini and O. Dulieu, Phys. Chem. Chem. Phys. **13**, 18905 (2011).

(20) P. Zabawa *et al*., Phys. Rev. A **82**, 040501 (2010).

(21) M. Bellos *et al.*, Phys. Chem. Chem. Phys. **13**, 1880 (2011).

(22) U. Gaubatz *et al.*, Chem. Phys. Lett. **149**, 463 (1988).

(23) P. Pellegrini *et al.*, Phys. Rev. Lett. **101**, 053201 (2008).

(24) W. C. Stwalley *et al.*, J. Phys. Chem. A **114**, 81 (2010).

(25) M. Debatin *et al.*, Phys. Chem. Chem. Phys. **13**, 18926 (2011).

(26) J. G. Danzl *et al*., Nature Physics **6**, 265 (2010).

(27) K. Winkler *et al.*, Phys. Rev. Lett. **98**, 043201 (2007).

(28) M. Viteau *et al.*, Phys. Rev. A **79**, 021402(R) (2009).

(29) Y. Lee *et al.,* J. Phys. Chem. A **112**, 7214 (2008).

(30) Y. Lee *et al.,* J. Phys. Chem. A **113**, 12187 (2009).

(31) Y. Lee *et al.*, J. Phys. Chem. A **114**, 7742 (2010).

(32) Y. Lee *et al.*, J. Chem. Phys. **115**, 7413 (2001).

(33) S. Rousseau, A. R. Allouche, and M. Aubert-Frecon, J. Mol. Spectrosc. **203**, 235 (2000).

(34) H. Lefebvre-Brion and R. W. Field, The Spectra and Dynamics of Diatomic Molecules (Elsevier: New York, 2004).

(35) J. T. Kim *et al.*, Phys. Chem. Chem. Phys. **13**, 18755 (2011).

(36) N. Okada *et al.*, J. Chem. Phys. **105**, 3458 (1999).

(37) S. Kasahara *et al.*, J. Chem. Phys. **111**, 8857 (1999).

(38) R. Beuc *et al.*, J. Phys. B: At. Mol. Opt. Phys. **39**, S1191 (2006).

(39) L. Pashov *et al.*, Phys. Rev. A **76**, 022511 (2007).

(40) D. Wang *et al*., Phys. Rev. A **75**, 032511 (2007).

(41) D. DeMille, Private communication (2011).

(42) K. Aikawa *et al.,* Phys. Rev. Lett. **105**, 203001 (2010).

(Color Online)

Fig. 1. The relevant *ab initio* PECs, primary energy levels and processes involved in this paper: a. PA from colliding K + Rb atoms to a bound electronically excited state e with rovibrational quantum numbers v, J, followed by SE to the weakly bound a state with rovibrational quantum numbers v, J; b. Absorption from UM in the weakly bound a state to an excited state $e'(v', J')$ (which may be different from the excited state reached by PA); c. Absorption from cold molecules in a supersonic MB in the X state with rovibrational quantum numbers $v'' = 0, J'' = 0,1,\cdots$; d. SRT combines the MB and UM transitions: SR1 and SR2 take population from the weakly-bound $a(v, J)$ states to $X(0, 0)$ via the $e'(v', J')$ intermediate state; e. RE2PI detection of the X and a state levels is usually through higher electronic states to the molecular ion ground state.

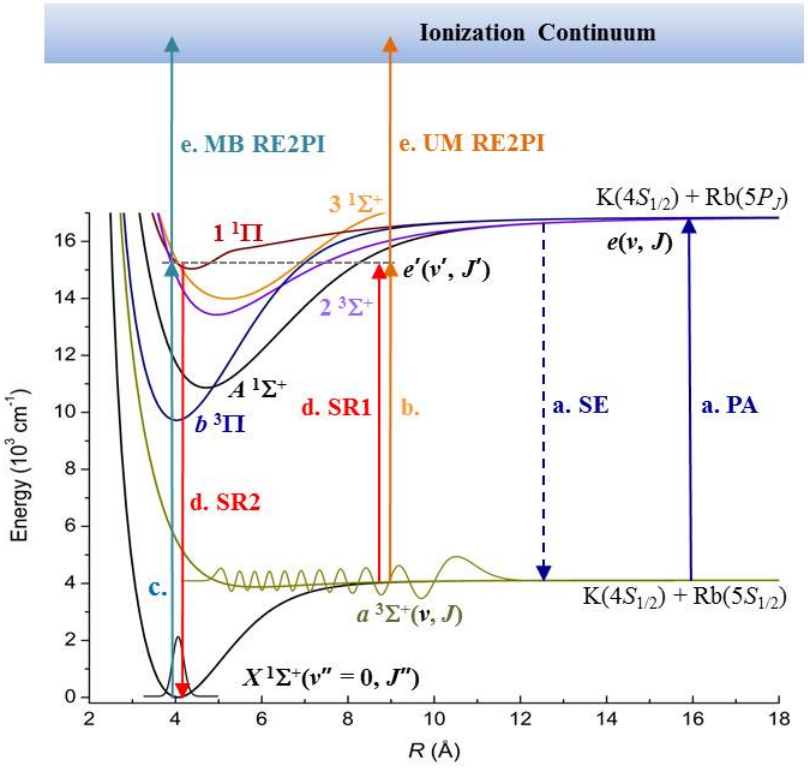

(Color Online)

Fig. 2. (a) MB, (b) UM, and (c) product between MB and UM spectra in the region 15372 – 15562 cm^{-1}. Assignments of the excited states such as $1\,^1\Pi_1$, $b\,^3\Pi_{0^\pm}$, $b\,^3\Pi_1$, $b\,^3\Pi_2$, $2\,^3\Sigma_1^+$, and $2\,^3\Sigma_{0^-}^+$ have been made, as reported in detail elsewhere [35]. The pairs of lines marked with symbol (?) are not assigned and the single line marked with symbol (+) is also unassigned. The very weak lines of the $3\,^1\Sigma^+$ state have recently been assigned. The *X* state molecules probed in the MB experiment are primarily in $v'' = 0$ and 1, split by 75.38 cm^{-1}, which are labeled by vertical solid and dashed lines in the MB spectra, respectively. The *a* state molecules probed in the UM experiment are mainly in v = 20 and 21, split by 4.23 cm^{-1}, which are labeled by vertical dashed and solid lines in the UM spectra, respectively. The energy shown is the energy with respect to the $X(0, 0)$ level, so the UM spectrum has been shifted by the energy of the *a* state v = 21 level. The strongest products (MB×UM), indicated by α, β, γ, and δ, are the optimal pathways for SRT, as discussed in the text.

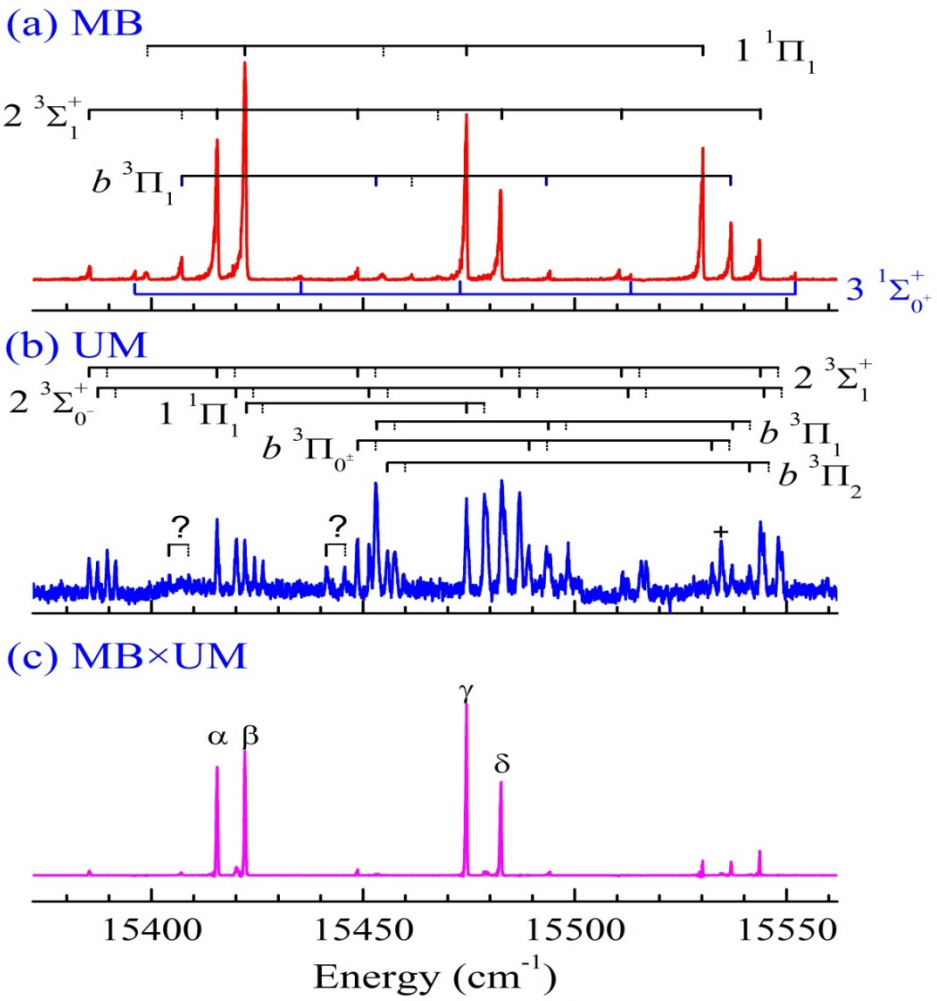

(Color Online)

Fig. 3. From comparison of the rotational contour fit of the $1\,^1\Pi\,(v'=11) \leftarrow X\,^1\Sigma^+\,(v''=0)$ band observed in our MB RE2PI spectrum from MB and the simulated spectrum, we fitted the following parameters: $T_{rot.}$ = 1.490(49) K, Gaussian linewidth = 0.1111(36) cm^{-1}, band origin = 15677.1992(31) cm^{-1}, and rotational constant = 0.02722(13) cm^{-1}. The P-, Q-, and R-branch rotational line positions are also shown.

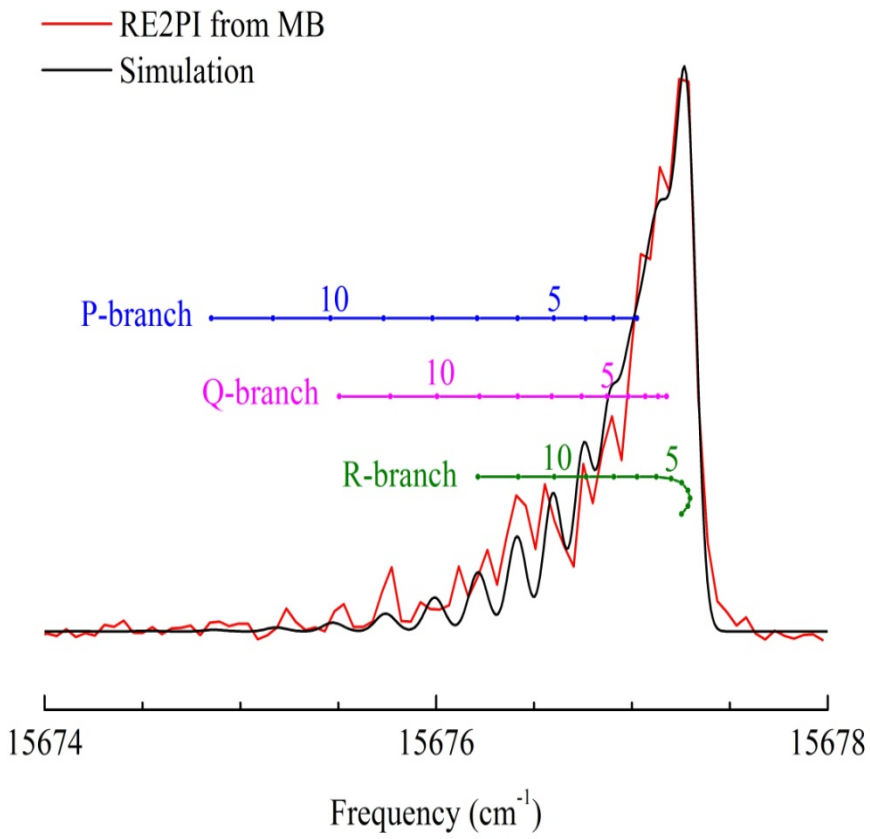

(Color Online)

Fig. 4. Vibrational intervals $\Delta G_{v'+1/2}$ as a function of $T_{v'}$ for (a) the $1\,^1\Pi$ state, and (b) the $2\,^3\Sigma^+$ ($\Omega=1$) and $b\,^3\Pi$ ($\Omega=1$) states. The perturbed $v'=7$ and 8 levels in (a), corresponding to the arrow, prove to be the optimal SRT routes because of their strongly mixed singlet-triplet character.